A CRISIS OF CONFIDENCE: THE COUNTERPARTY-LIQUIDITY RISK NEXUS IN AN AGENT-BASED NETWORK MODEL OF THE INTERBANK MARKET*

Job Market Paper

Nicolas K. Scholtes†

Preliminary draft. Please do not cite or distribute

May 30, 2016

Abstract

This paper provides a behavioural motivation for the interbank market downturn that occurred during the global financial crisis. Two types of interdependency, represented in a counterfactually simulated *bilayer* network model are considered namely, *direct exposures* arising due to borrowing/lending behaviour of banks on the interbank market and *indirect exposures* in which banks are linked due to commonly-held securities/overlapping portfolios. Embedded in both layers of the simulated network, we develop an Agent-Based Model whereby banks use adaptive expectations in the form of simple heuristics to fix interbank borrowing/lending volumes, set interbank rates and sell off their securities to meet obligations to creditors and/or macroprudential policy constraints. The crux of the model involves banks' setting of interbank rate risk premia stemming from counterparty, funding and market liquidity risk.

Keywords: Interbank network, Agent-Based Computational Economics, financial stability, contagion, macroprudential policy

JEL Classification: C63, G01, E03

*The author acknowledges support of the "Communauté francaise de Belgique" through contract "Projet d'Actions de Recherche Concertées "13/17-055" (Financial CompleX Systems) granted by the Académie universitaire Louvain. We thank participants at the NIAS-Lorentz workshop on socio-economic complexity and the 2015 Spring Meeting of Young Economists. The usual disclaimer applies.

†CORE, Université catholique de Louvain & CeReFiM, Université de Namur.

E-mail address: nicolas.scholtes@unamur.be

1 Introduction

A key feature of the 2008-2009 global financial crisis (GFC) was the resulting impairment or drying up of global money markets. Observing this, US Federal Reserve officials noted that "*...banks took measures to conserve their liquidity and were cautious about counterparties' exposures to asset-backed commercial paper. Term interbank funding markets were significantly impaired, with rates rising well above expected future overnight rates and traders reporting a substantial drop in the availability of term funding*".[1] Given the importance of interbank markets in providing private sector credit and as the first step in the transmission mechanism of monetary policy, central banks worldwide were quick to intervene by proactively injecting liquidity into the banking system in order to restore its normal functioning.

Following this global policy response, interbank rate dynamics received renewed attention as researchers sought to determine the possible mitigating effects of central bank liquidity-providing operations as well as identify the main risks that exacerbated interbank market tensions in the first place. The majority of papers in this strand of the literature agree that liquidity hoarding by banks and increases in interbank rate spreads were the primary consequences of the GFC's manifestation in the interbank market. However, they differ in their assessment of the underlying *causes* of the aforementioned *effects*. Specifically, the debate has focussed primarily on the identification and modelling of credit and liquidity factors, their interplay and resulting effect on interbank market dynamics.

From a theoretical standpoint , Heider et al. (2015) develop a model in which the interplay between endogenous liquidity and asymmetric information about the risk of banks' assets exacerbates *counterparty credit risk*[2] and can lead to liquidity hoarding behaviour. By contrast, Eisenschmidt and Tapking (2009) argue that counterparty risk alone cannot account for the increased spreads in the unsecured interbank market. They identify a *funding liquidity risk premium* whereby banks lend at elevated rates in term money markets in order to account for the risk of borrowing in the overnight segment. Within the empirical literature, both Michaud and Upper (2008) and Schwarz (2015) Ait-Sahalia et al. (2012) find that while Taylor and Williams (2009).

As the above indicates, there is no general consensus on the the mechanisms underpinning liquidity hoarding as well as the main determinants of interbank rate dynamics and consequently, how central banks can optimally set policy while accounting for risks to financial stability. This paper provides an attempt to resolve this by applying novel tools from the network theory and Agent-Based Computational Economics (ACE) literature. Specifically, our approach entails embedding a *multi-agent* (MA) model inside a network calibrated to replicate certain topological regularities of real interbank networks. Where the network determines the initial set of interdependencies between banks, the MA model dictates how banks interact with one another in this

[1] Minutes of the FOMC, September 18th, 2007. Available at http://www.federalreserve.gov/fomc/minutes/20070918.htm

[2] Indeed, (Jorion and Zhang, 2009) observe that the Lehman Brothers default in September 2008 was exacerbated by

environment by fixing interbank borrowing/lending volumes as well as interest rates.

Our theoretical approach is based on two premises. First, we justify our use of an exogenously-imposed, static network structure[3] by citing the literature on *relationship lending* between banks. Specifically, a number of empirical studies find that banks engage in long-term, stable relationships with one another. Evidence of such relationships has been found in the Portuguese (Cocco et al., 2009) interbank market and overnight loans in the U.S Fedwire payment system Afonso et al. (2013).

As pointed out in Brunnermeier and Pedersen (2009), the interplay between traders' funding liquidity and the market liquidity of assets

Our paper contributes to this literature by modelling interbank lending/borrowing and rate setting behaviour within the framework of an Agent-Based Model (ABM) wherein agents' use simple heuristics based solely on past actions on the interbank market of its counterparties to set

The ABM is embedded in a network calibrated to replicate topological regularities of real interbank networks. Networks provide an intuitive framework for studying interbank markets (Allen and Babus (2009); Schweitzer et al. (2009)) due to their ability to incorporate heterogenous banks (modelled as *nodes*), various types of mutual interaction (by defining the *edges* connecting nodes) as well as the strength of the interactions (for example, lending volumes which are captured by the *weight* associated to each edge). Expanding on the *static* framework provided by the network, the ABM allows us to construct a dynamic model in which large-scale properties (referred to as *emergent phenomena* in the complex systems literature) arise as the result of the behaviour of locally interacting agents (Axelrod, 1997)[4]. As we will show, the emergent phenomenon we extract from interbank market dynamics is precisely the "*behaviour under stress of a complex, adaptive network*" (Haldane, 2009) observed during the crisis.

The model proceeds in two steps. We begin by counterfactually simulating a *core-periphery* network of direct interbank exposures[5] using calibrations from past studies on bank size heterogeneity[6] as well as the degree-distribution and assortativity of national banking systems. Using a matching algorithm derived from Montagna and Lux (2013), wherein the probability that two banks form a link is determined by the product of their relative sizes[7], we generate an undirected, unweighted network that prescribes the initial set of *relationships* between banks[8]. In addition,

[3] As opposed to the *endogenous networks* literature focussing on network formation games.

[4] For arguments on the advantages of ABM, the interested reader is referred to works by Tesfatsion and Judd (2006), Colander et al. (2008) and Farmer and Foley (2009).

[5] Recent papers mapping various interbank networks have found this to be the prevailing topology. Examples include Craig and Von Peter (2014), Fricke and Lux (2014), in't Veld and van Lelyveld (2014) and Langfield et al. (2014) using German, Italian e-MID, Dutch and UK data, respectively. Regarding the degree-distribution, several studies find that interbank networks are scale-free. These include (Boss et al., 2004), (Soramäki et al., 2007), (Bech and Atalay, 2010) and (Iori et al., 2008) for the Austrian interbank market, the US Fedwire network, the US Federal funds market and the Italian e-MID dataset, respectively

[6] Though less studied than network properties, empirical papers on bank size distribution in the US (**?**) and globally (**?**) show that bank sizes are distributed according to a power law

[7] Also referred to as *node fitness* in Caldarelli et al. (2002) who initially developed the approach, referred to as the *fitness-based model with mutual benefit*.

[8] Several empirical studies have found that bank relationships are an important determinant of interbank market

we incorporate the recent observation by Upper (2011) and Summer (2013) that direct exposures alone are not a significant contributor to systemic risk by also allowing banks to hold overlapping portfolios of securities, thus providing a form of *indirect* dependency between banks via the endogoneous dynamics of the securities within their portfolios.

Once the network has been generated, we embed the ABM using the approach developed by Lux (2015) where the balance sheet elements of each heterogeneous bank are derived using the bank sizes and a set of calibrated weight parameters. Once bank balance sheets have been initialised, the ABM is allowed to run over a fixed simulation time, with each period comprising two phases in which various aspects of interbank trading occur. In phase 1, a deposit shock determines whether banks go to the interbank market as *lenders* or *borrowers*. Notice that this also switches the initial undirected network to a directed one. In our model, borrowers (those hit by a negative shock) begin by making requests to their local neighbourhood of counterparties. This stage features two key components: (i) A calibrated interbank market transparency parameter to determine whether borrowers are aware of the shock sign distribution and (ii) a *risk adjustment factor* in which borrowers target lenders who, in past simulation periods, have provided liquidity at a reasonable interest rate.

Once borrower requests have been set, lenders allocate available liquidity across their counterparties and, in the main component of the model, fix the interbank rate offered to each borrowing counterparty. Our approach in this stage relies on the fact that each period features a new liquidity shock and thus, a new set of lenders and borrowers on the interbank market. We develop a framework by which the rate set by the *lender* is decomposed into a counterparty risk component (based on borrowers' past repayment of their loans), a funding liquidity risk component (based on past lending behaviour of current borrowers) and a market liquidity risk component (based on the price dynamics of the assets held in the lender's portfolio). These components are then combined in the final bilateral interest rates of each lender using a weighting scheme across the three components. We develop a reinforcement learning mechanism by which lenders vary the weights depending on the future rewards of a particular weighting scheme.

Following the transferral of liquidity from lenders to borrowers, in the next step all banks are subject to an exogenous shock to their external asset portfolios. This affects borrowers ability to repay their loans set in the previous phase. To this end, they sell off a fraction of their portfolio in order to (ii) meet their interbank obligations and (ii) ensure that macroprudential constraints on liquidity and capital are met. Using the mechanism developed in Cifuentes et al. (2005) and expanded in **?**, second-round effects in asset prices are triggered.

The paper is organised as follow: Section 2 constructs the algorithms used to generate each layer of the multilayer network, section 3 describes the dynamic agent-based model and endogenous price-adjustment mechanism embedded in each layer of the network, section 4 outlines the simulation methodology and generated networks, section 5 provides the results of the simulations and section 6 concludes and provides policy recommendations based on our findings.

dynamics (Cocco et al., 2009)

2 Related literature

From a methodological perspective, our paper draws on the literature extending the static network representation by allowing banks to respond to their environment using either a strategic[9] or a heuristic-based[10] decision rule. Most similar to our approach is the paper by **?** who study a *multilayer* embedding an ABM in which agents adjust their balance sheets after exogenous shocks drive their liquidity or capital ratios below regulatory requirements. Our treatment of interbank *confidence* is similar to the notion of trust developed in Lux (2015) which provides the reinforcement-learning mechanism that strengthens/weakens existing relationships between banks. However our formulation differentiates between *lender* and *borrower* confidence in order to encapsulate counterparty and funding liquidity risk respectively. Iori et al. (2015) use a proxy for trust which is also based on repeated interactions between banks. The dynamic aspect of our model is similar to **?** who develops a multi-agent simulation with portfolio-optimising banks engaging in bilateral interbank lending which occurs through a credit rationing mechanism[11] An ABM with strategic interactions is developed in **?** who treat bilateral exposures as the outcome of a sequential optimisation process played by individual banks whereby banks meet in a bargaining game in which the supply and demand for interbank lending is determined. Their ABM is also embedded in a simulated network, in their case based on the *probability map* developed in **?**.

The emergency liquidation/fire sale mechanism we incorporate as an amplification mechanism is based on a form of 'cash-in-the-market' pricing which was first applied to fire-sale induced contagion in interbank markets by Cifuentes et al. (2005). This has been applied in a simplified context in the network models of Nier et al. (2007) and Gai and Kapadia (2010) both finding that interactions between liquidity effects and the banking system result in a higher probability of systemic breakdown. Their approach is integrated into the static network models of Nier et al. (2007) and Gai and Kapadia (2010), both finding that interactions between liquidity effects and the banking system result in a higher probability of systemic breakdown. More recently, multiple external asset holdings are considered inCaccioli et al. (2014), **?** and Huang et al. (2013), thereby allowing individual bank portfolios to *overlap* to varying degrees. The authors find that the interplay between the two channels results in a contagion process that mirrors the asset market liquidity and bank funding liquidity framework of Geanakoplos (2010) and Brunnermeier and

[9] Given that our own approach develops an ABM of interbank networks, we abstract from a comprehensive review of the *strategic* (i.e. game-theoretic) literature. Key papers include Acemoglu et al. (2015) who identify a *financial network externality* when banks are allowed to lend to each other through debt contracts, **?** who propose a strategic game à-la Cournot to identify the equilibrium amount of lending due to the network structure and **?** in which optimising banks undertake an optimal portfolio allocation by maximising profits subject to liquidity and capital requirement constraints.

[10] Our model is based on the latter: Bank behaviour is myopic, non-rational and captured by a set of behavioural heuristics. As mentioned in Anand et al. (2013), such models are at odds with much of the current literature on financial networks but allow for an integrated model of systemic risk given that the heuristics capture bank behavioural responses in a plausible manner.

[11] This mechanism does not *a priori* allow for interbank market-clearing. However, their rationing mechanism allows banks to approach the central bank for liquidity and differentiates between planned investment levels and realised ones. Our approach differs by forcing market-clearing through borrower-induced firesales.

Pedersen (2009). In the absence of the granular data required to reconstruct such networks, most papers turn to simplifying assumptions whereby either a single asset is held (as in the recent paper by Caccioli et al. (2015)), or the bipartite network is constructed randomly.

3 Simulating the bilayer network

Before developing the dynamic portion of the model, we first develop the methodology for simulating a bilayer network while satisfying the topological properties of interbank networks mentioned earlier. Bilayer networks consider two *different* types of interdependency connecting the *same* set of nodes. In our model, the two forms of bank interdependency are (i) direct exposures due to short-term, unsecured interbank lending/borrowing and (ii) indirect exposures arising due to overlapping portfolios and firesales of securities held within those portfolios. Moreover, our framework allows for transmission and feedback effects between the two layers as banks' activities vis-à-vis their counterparties on the interbank market condition their need to firesale assets in their portfolio and vice versa.

3.1 Interbank network

3.1.1 Definitions

In this section, we develop the theory behind our simulation of short-term, unsecured interbank markets. Relying on the assumption that banks establish long-term *relationships* with certain counterparties, we justify our methodology in which the network is generated exogenously and prior to the running of the embedded ABM.

The initial direct exposure network is an *unweighted, undirected* graph (also referred to as a *simple* graph), $\mathcal{G}^{IB}(\mathcal{N}, \mathcal{E})$ comprising node set $\mathcal{N}$ and the edge set $\mathcal{E}$ containing all unordered pairs of connected nodes, $\mathcal{E} \subseteq \mathcal{N}^2$. The number of nodes in the network N is given by the cardinality of $\mathcal{N}$. In our model, nodes represent banks while the edges determine the presence of a pre-existing lending/borrowing relationship. Intuitively, such a relationship should be *directed* in order to reflect the difference between node i lending to or borrowing from j. Indeed, our model allows for oriented edges between banks though we incorporate these into the ABM wherein an undirected edge between banks is transformed to a directed one depending on the bank's role as a supplier or demander of liquidity in the transaction[12]. In this way, our approach is more flexible than those assuming fixed directed edges between banks.

The network is represented by the symmetric, binary *adjacency* matrix $[a_{ij}]_{N\times N} = \mathcal{A}(\mathcal{G}^{IB})$ where $a_{ij} = 1$ if there exists an edge connecting i and j and $a_{ij} = 0$ otherwise. Similarly, our simple graph model precludes the presence of self-loops ($a_{ii} = 0$) and multi-edges ($a_{ij} > 1$). Consequently, the maximum number of edges possible in such a network is given by $N(N-1)/2$.

[12]Moreover, undirected edges can also be interpreted as being *bidirectional* i.e. encompassing a directed edge from i to j and from j to i.

3.1.2 Simulation

We assume that intrinsic fitness of each bank $i \in \mathcal{N}$ stems from the total assets a_i, of the bank. Consequently, large banks (that is, banks holding a large number of assets on their balance sheets) are more likely to connect with large banks than small banks due to the aforementioned fitness-based model. The first step is thus to populate the node set with N banks. This is done using the following *truncated power law*:

$$f(a; \gamma_a, a_{min}, a_{max}) = \frac{(1-\gamma_a)}{a_{max}^{1-\gamma_a} - a_{min}^{1-\gamma_a}} a^{-\gamma_a} \tag{1}$$

Where γ_a is an exogenous parameter dictating the shape of the power law distribution and a_{min} and a_{max} represent the smallest and largest banks in the system, respectively. This determines the initial (i.e. at time $t = 0$) size of each bank i in the system. We denote this by a_i^0. These values are then passed to the following function which gives the probability, p_{ij} of an undirected edge existing between i and j Dropping the 0 superscript for simplicity, the probability function is given by:

$$p_{ij} = P(a_i, a_j) = \left(\frac{a_i}{a_{max}}\right) \cdot \left(\frac{a_j}{a_{max}}\right) \tag{2}$$

The adjacency matrix is then constructed according to the following rule:

$$a_{ij} = \begin{cases} 1, \text{ with probability } p_{ij} \\ 0, \text{ with probability } 1 - p_{ij} \end{cases} \tag{3}$$

Note that the original fitness-based model with mutual benefit proposed in Caldarelli et al. (2002) and applied in Montagna and Lux (2013) simulates a directed network with the network structure relying on two calibrated exponents, $\{\alpha, \beta\}$. The undirected version in our model involves setting $\alpha = \beta = 1$. Moreover, the model is known to produce a scale-free degree distribution with the value of the exponent depending on the α and β. Under our calibration, we obtain a theoretical degree distribution, $p(k) \propto k^{-2}$ which is consistent with numerous empirical findings of interbank network structure.

3.2 Overlapping portfolio network

3.2.1 Definitions

The network given by $\mathcal{G}^{\mathcal{OP}}(\mathcal{N}, \mathcal{M}, \mathcal{E})$ comprises the same set of nodes $\mathcal{N}$ whose interdependence in this layer arises *indirectly* via the degree of overlap in their external asset portfolios. The set of external assets is given by $\mathcal{M}$ whose cardinality, M is the total number of assets across all banks. The notion of a *bipartite network* from the graph theory literature offers an ideal representation.

Figure 1: Bipartite network representing banks' (blue circles) common holdings of external assets (red squares)

Specifically, this framework allows for two distinct types of nodes (defined by the disjoint sets $\mathcal{N}$ and $\mathcal{M}$ above) where edges are only permitted between nodes in different sets. Mathematically, the elements of the adjacency matrix $\left[a_{ij}^{OP}\right]_{N\times M} = A\left(\mathcal{G}^{\mathcal{OP}}\right)$ are equal to 1 if there exists a link between $i \in \mathcal{N}$ and $j \in \mathcal{M}$ and 0 otherwise.

Following Caccioli et al. (2014), we provide a set of parameters associated to the bipartite network. First, the *average diversification* of the banks is the average number of assets held by each bank $i \in \mathcal{N}$ given by its degree, deg_i^{OP}.

$$\mu_b = \frac{1}{N}\sum_{j=1}^{N} deg_i^{OP} \tag{4}$$

Similarly, the degree of each asset $j \in \mathcal{M}$ represents the number of banks holding it in their portfolio. The average degree is thus given by:

$$\mu_a = \frac{1}{M}\sum_{i=1}^{M} deg_j^{OP} \tag{5}$$

Since the total degrees of both banks and external assets must match, the following condition must hold

$$\mu_b N = \mu_a M \tag{6}$$

In order to define the degree of overlap between banks, the *crowding parameter*, $n = N/M$ measures the extent to which banks' portfolios contain the same assets. Finally, We denote the total value of external assets held by bank i in period t by

$$e_i^t = \sum_{\text{J}=1}^{M} s_{ij}^t \cdot p_j^t, \quad \forall i \in \mathcal{N} \tag{7}$$

Where s_{ij}^t denotes the number of shares of asset j held by bank i and p_j^t the price of asset j at time t. Note that s_{ij}^t is nonzero if bank i holds asset j in its portfolio. Grouping terms, we define the $1 \times M$ asset vector of bank i, $s_i^t = [s_{i1}^t, \ldots s_{iM}^t]$ along with the $[1 \times M]$ price vector

$p^t = [p_1^t, \dots p_M^t]$.

In order to track portfolio dynamics, we define the $N \times M$ external asset matrix:

$$S^t = \begin{pmatrix} s_{11}^t & \dots & s_{1M}^t \\ s_{21}^t & \dots & s_{2M}^t \\ \vdots & \ddots & \vdots \\ s_{N1}^t & \dots & s_{NM}^t \end{pmatrix} \tag{8}$$

Using the above formulation, Equation 7 can be expressed in vector terms as $e^t = S^t \cdot p^{t\prime}$

3.2.2 Simulation

Keeping to the framework developed by Caccioli et al. (2014), we consider random networks with Poisson degree distribution for both banks and external assets. Consequently, the probability of a link being formed between each bank-asset pair is given by $\frac{\mu_b}{M}$. The result is an Erdős-Renyi graph with average degrees for banks and assets given by μ_b and $\mu_a = \mu_b \cdot \frac{N}{M}$, respectively

4 The Model

4.1 Initialisation

Following Lux (2015), we create the initial entries of the balance sheet using the N bank size values drawn in the previous section:

$$\begin{aligned} e_i^0 &= \alpha a_i, \; c_i^0 = (1-\alpha) a_i^0 \\ d_i^0 &= \beta a_i^0, \; k_i^0 = (1-\beta) a_i^0 \end{aligned}$$

Where e_i^0 and c_i^0 respectively represent external asset and cash holdings on the asset-side of i's balance sheet at $t = 0$ while initial liabilities comprise deposits d_i^0 and capital k_i^0. α, β are calibrated parameters representing the initial fraction of external assets and deposits respectively. The above implies that $l_i^0 = b_i^0 = 0$ i.e. no interbank lending exists ex-ante. Rather, the interbank market arises endogenously due to the shocks and ensuing liquidity positions of banks in the network.

Recall that our assumption of relationship between banks involves each $i \in \mathcal{N}$ having a *local neighbourhood* of counterparties with whom it engages in lending/borrowing on the interbank market. We denote i's set of counterparties by $\mathcal{N}_i$. The number of i's counterparties is determined from node i's *degree*[13], $|\mathcal{N}_i| = N_i = deg_i^{IB} = \sum_{j=1}^{N} a_{ij}$.

[13] See Appendix 7 for an overview of the network measures used in this paper

In order to allow for heterogeneity as well as overlap in banks' asset portfolios, we assume that initially, the market prices of the M assets held by each bank are identical and equal to one viz. $p^0 = \mathbf{1}$ where $\mathbf{1}$ is an M-dimensional vector. As a result, i portfolio is equally-weighted with $s_\mu^{i,0} = \frac{e_i^0}{M}$ where e_i^0 is set exogenously in Section 4.3 as a linear function of a_i^0. This formulation implies that larger banks will ex ante have larger securities portfolios as a whole as well as hold a larger amount of each of the securities.

4.2 Balance sheet

The asset side of the stylised balance sheet comprises cash reserves, c_i, interbank loans, l_i and securities holdings, e_i. At each period, the balance sheet identity requires that this equals liabilities, comprising customer deposits d_i, interbank borrowing b_i and bank capital k_i. That is,

$$\begin{aligned} a_i &= e_i + l_i + c_i \\ i_i &= d_i + b_i + k_i \end{aligned}$$

Figure 2 provides a simple schematic with 2 banks of differing size connected directly via the larger bank lending to the smaller and indirectly via three commonly-held securities.

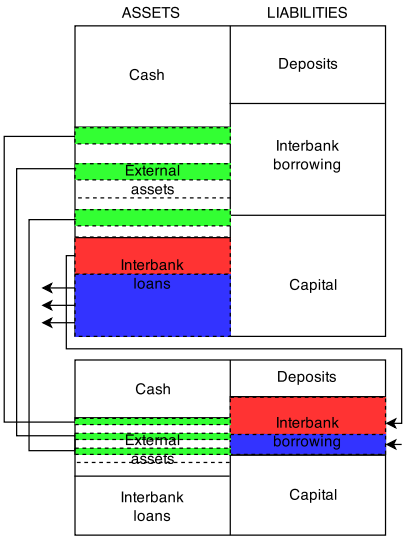

Figure 2: Interlocking balance sheets with 2 banks

Recall that these two forms of interdependency arise from the bilayer network simulated in the previous section.

4.3 Dynamic model

One of the key points of the dynamic model is the evolution of the balance sheet over time. In order to provide a realistic depiction of interbank market activity, we consider a temporal structure consisting of $t = 1, \ldots T$ *periods* in simulation-time, each of which comprises $\tau = 2$ *phases*. In order to highlight how certain parameters evolve over time, each variable is defined by a period-phase 2-tuple $\{t, \tau\}$.

Figure 3 below outlines the main dynamics of the ABM as well as the ordering in which agents interact with one another. Specifically, the arrows labelled with a diamond provide the key mechanisms dictating how agents' actions in the previous period (indicated by the tail of the arrow) affects actions either in the same phase (arrows 1 and 2) or in the other phase (arrows 3-5) of the current period (indicated by the head of the arrow). For example, the arrow labelled 1 indicates that the lender's bilateral rate setting behaviour in phase 1 of of period $t-1$ affects its borrowing counterparty's risk adjustment in period t. Similarly, arrow 5 states that firesales conducted by borrowers in order to refinance their interbank loans in phase 2 of period $t-1$ affects the market liquidity risk component of lender interbank rate setting in phase 1 of period t.

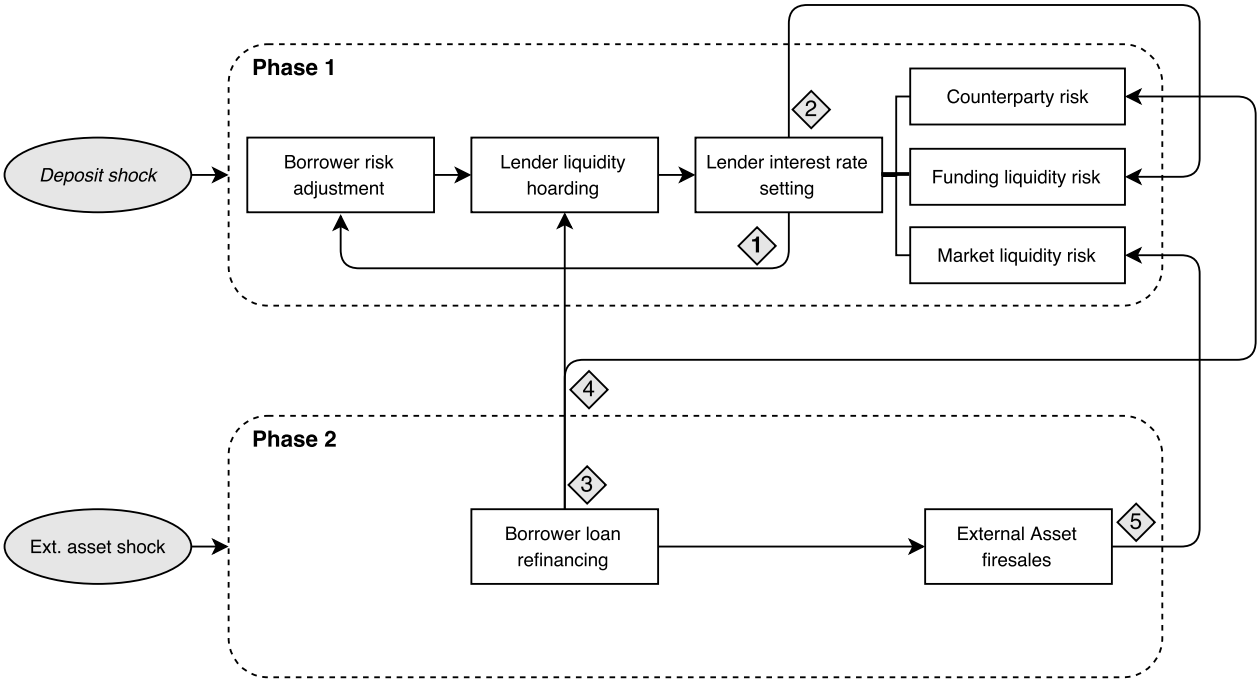

Figure 3: Agent-based model dynamics

4.3.1 Phase 0: Balance sheet updating

At the beginning of each period (phase 0), each bank's balance sheet comprises only variables carried over from the previous period (except at $t = 0$). All debt contracts are assumed to have been settled (fully or partially) in the previous period i.e. $l_i^{t,0} = b_i^{t,0} = 0$. As a result, the balance

sheet in phase 0 of period t is given by:

$$\begin{aligned} a_i^{t,0} &= c_i^{t-1,3} + e_i^{t-1,2} \\ i_i^{t,0} &= d_i^{t-1,1} + \tilde{k}_i^{t,0} \end{aligned}$$

Note that the first superscript in the two equations above indicates that the parameter was carried over from the previous period while the second indicates the intra-period phase in which the parameter was updated. Bank capital $\tilde{k}_i^{t,0}$ is a residual value, set such that $a_i^{t,0} = i_i^{t,0}$. Consequently, it can be expressed as:

$$\tilde{k}_i^{t,0} = c_i^{t-1,3} + e_i^{t-1,2} - d_i^{t-1,1} \tag{9}$$

4.3.2 Phase 1: Liquidity shock and move to interbank markets

Phase one begins with an idiosyncratic *liquidity shock* on bank deposits:

$$d_i^{t,1} = d_i^{t-1,1} + \Delta d_i^{t,1} \tag{10}$$

Where $\Delta d_i^{t,1} = \theta_i^{t,1} \cdot \epsilon$ and $\epsilon \sim \mathcal{N}(\mu^{\mathcal{F}}, \sigma^{\mathcal{F}})$ where $\mathcal{F} = \{stable, crisis\}$ are parameters that we will use to calibrate the size of the deposit shock and $\theta_i^{t,1} = f\left(a_i^{t,1}\right)$ is a *size multiplier* that controls for the fact that large banks hold more deposits and thus, are susceptible to larger deposit fluctuations. We choose the idiosyncratic component to be equal to the relative asset size of the bank:

$$\theta_i^{t,1} = \frac{a_i^{t,1}}{\sum_{j=1}^{N} a_j^{t,1}} \tag{11}$$

In our model banks play the traditional role of *maturity transformers*, using short-term deposits to finance long-term, illiquid investments. To this end, interbank market activity is initially driven by the magnitude and sign of the deposit shock, $\Delta d_i^{t,1}$. If i experiences a positive liquidity shock ($\Delta d_i^{t,1} > 0$), it uses that amount to finance an illiquid investment $z_i^t = \Delta d_i^{t,1}$ which pays a fixed interest rate r^z at the beginning of every period over the entire simulation. In addition, i assumes the role of *lender* on the interbank market, providing liquidity to banks experiencing a negative deposit shock, $\Delta d_i^{t,1} < 0$ in that period. These banks, desiring a similar investment opportunity, request $\tilde{b}_i^t = |\Delta d_i^{t,1}|$ on the interbank market in the form of borrowing[14] in order to overcome the

[14] $\tilde{b}_i^t$ indicates that these are *provisional* values. Since the actual interbank credit is decided by lenders (as will be seen), the final balance sheet component for interbank borrowing, b_i^t will depend on the loan-provision activities of

negative shock and make the investment $z_i^t = |\Delta d_i^{t,1}|$.

After fixing their aggregate liquidity needs, each borrower i now redistributes this value across their local neighbourhood of counterparties. The network structure comes into play at this point as the number of local counterparties, N_i determines the number of banks from whom they can request liquidity. Before proceeding with the model, we define a set of variables conditional on the realised shock distribution. First, the set of banks hit by a negative shock in t, $\mathcal{N}_-^t = \left\{j \in \mathcal{N} : \Delta d_j^t < 0\right\}$ and its complement corresponding to banks hit by a positive shock, $\mathcal{N}_+^t = \mathcal{N} \backslash \mathcal{N}_-^t$. This allows us to refine the set of each bank's local counterparties according to their status *viz.* $\mathcal{N}_-^t \supseteq \mathcal{N}_{i,-}^t = \left\{j \in \mathcal{N}_i : \Delta d_j^t < 0\right\}$ and $\mathcal{N}_+^t = \mathcal{N}_i \backslash \mathcal{N}_-^t$.

In our framework, the realisation of the liquidity shock imposes directed edges on the previously undirected network as a request from bank j to bank i for liquidity implies a directed edge from i to j.[15] Since interbank transactions are *borrower-initiated* in our model, the head of a directed edge is placed *ex-post* at each node hit by a negative shock conditional on there being an undirected edge there *ex-ante* (signifying a pre-existing relationship between two banks).

We incorporate the notion of information asymmetry as a driver of interbank market tensions via the parameter $\Phi = \{I, P\}$ representing the *transparency* of the banking system. Specifically, it is defined as the ability of all banks to observe the shock sign realisation of their neighbours. In the case that $\Phi = I$ (imperfect transparency), borrowers request liquidity from counterparties also facing a liquidity deficit. Since our framework precludes banks hit by a negative shock from lending out liquidity, a zero loan in response to a nonzero request will have ramifications in future rounds of the simulation. Alternatively, when $\Phi = P$ (perfect transparency), borrowers are able to discern between banks with an *ex-post* liquidity surplus and deficit and target their requests towards the former.

Taking these rules into account, we populate the adjacency matrix of the directed network in period t[16] as follows:

$$\vec{a}_{ij}^{t,A} = \begin{cases} 1 \text{ if } j \in \mathcal{N}_-^t \wedge i \in \mathcal{N}_{j,+}^t \\ 1 \text{ if } j \in \mathcal{N}_-^t \wedge i \in \mathcal{N}_{j,-}^t \wedge \Phi = I \\ 0 \text{ if } j \in \mathcal{N}_-^t \wedge i \in \mathcal{N}_{j,-}^t \wedge \Phi = P \\ 0 \text{ otherwise} \end{cases}, \quad \forall i, j \in \mathcal{N} \tag{12}$$

Figure 4 illustrates this using a simple six-node network. When $\Phi = I$, borrower 2 is unable to discern that its counterparties 4 and 6 are also facing a liquidity deficit hence the directed edge between 2 and 4 and 2 and 6. By contrast, when $\Phi = P$ 2 no longer requests liquidity from 4 and 6, recognising their status as interbank borrowers.

In order to determine bilateral loan requests of borrowers to their creditors, we assume that they

lenders.

[15] This is conventional in directed financial networks as it represents a flow of funds from lender i to borrower j.

[16] Notice that the structure of the directed network will thus depend on the realisation of the liquidity shock and thus, will vary from period-to-period.

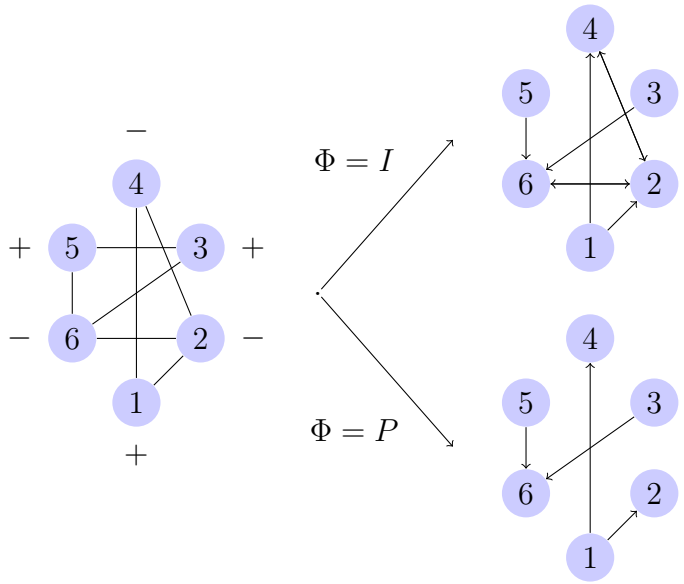

Figure 4: Revealing the directed network conditional on shock sign distribution under imperfect ($\Phi = I$) and perfect ($\Phi = P$) interbank market transparency

initially redistribute their aggregate loan requests, $\tilde{b}_i^t$ *equally* across their counterparties. Thus, bilateral requests $\tilde{b}_{ij}^t$ are given by $\left(\frac{1}{N_i}\right)\cdot\tilde{b}_i^t$ or $\left(\frac{1}{N_i^+}\right)\cdot\tilde{b}_i^t$ when Φ equals I or P, respectively. We now introduce the first backward-looking heuristic by allowing borrowers to reallocate loan requests based on past behaviour of their creditors. Specifically, we define a *rollover risk adjustment* whereby borrowers in the current period t begin by looking backwards to the *last* period in which a negative shock cast them as borrowers, defined by $\hat{t}_i^B = \sup\{\hat{t} \in t-1 | \Delta d_i^{\hat{t}} < 0\}$. Using the equally-weighted bilateral requests determined above as a benchmark, borrowers proceed to divert loan requests away from creditors displaying a higher rollover risk i.e. who are more unlikely to provide funding at a reasonable rate. Using its observation of creditor behaviour in $\hat{t}_i^B$, each borrower recomputes its bilateral requests according to:

$$\begin{aligned} b_{ij}^t &= \mathbb{1}_{\left\{j\in\mathcal{N}_i | r_{ji}^{\hat{t}_i^B} \leq \bar{r}_{ji}^{\hat{t}_i^B}\right\}} \cdot \left[\tilde{b}_{ij}^t + \psi_i^t \left| r_{ji}^{\hat{t}_i^B} - \bar{r}_{ji}^{\hat{t}_i^B} \right|\right] \\ &- \mathbb{1}_{\left\{j\in\mathcal{N}_i | r_{ji}^{\hat{t}_i^B} > \bar{r}_{ji}^{\hat{t}_i^B}\right\}} \cdot \left[\tilde{b}_{ij}^t - \psi_i^t \left(r_{ji}^{\hat{t}_i^B} - \bar{r}_{ji}^{\hat{t}_i^B} \right)\right], \forall i \in \mathcal{N}_-^t \end{aligned} \tag{13}$$

where $\mathbb{1}_{\{\cdot\}}$ denotes the indicator function defined on the set of borrower i's counterparties. Under this framework, i proceeds to defining two disjoint sets, each containing its lenders whose past interbank rate was less than or greater than the mean across lenders. In this way, borrowers incorporate past behaviour of creditors when allocating liquidity requests by shifting the (former) equal-weights towards counterparties providing a comparatively more favourable interbank rate. The dynamics of Equation 13 can be described as follows: For lenders lending at a rate *lower* than the average, borrowers increase the initial request b_{ij}^t by an amount proportional to the absolute

difference between the bilateral and average interbank rate. Thus, lenders offering the lowest rates in the past are subject to higher liquidity requests in the current period. The same logic applies to the set of lenders offering higher rates than the mean. In this case borrowers reduce their bilateral liquidity requests further as lenders' past rates diverge from the mean. Note that in both cases, the extent of borrowers' response to past interbank rates is driven by the parameter ψ_i^t which we hereafter refer to as the *rollover risk adjustment factor* and denotes the degree of borrower responsiveness to past lender behaviour. We assume that it is driven by the change in realised liquidity shock magnitude between the current period t and the last period in which i was cast as a borrower, $\hat{t}_i^B$:

$$\psi_i^t = \psi_i^{t-1} \cdot \frac{\Delta d_i^t}{\Delta d_i^{t-1}} \tag{14}$$

Equation 13 can be represented by the following schematic where (a) and (b) correspond respectively to the first and second lines. Taking (a) as an example, the provisional request $\tilde{b}_{ij}^t$ is captured in the intercept where $b_{ij}^t = \tilde{b}_{ij}^t$ when $\bar{r}_{ji}^{\hat{t},IB} = r_{ji}^{\hat{t},IB}$. Then, as bilateral rates *decrease* relative to the mean, borrowing requests increase proportional to the current value of ψ_i^t.

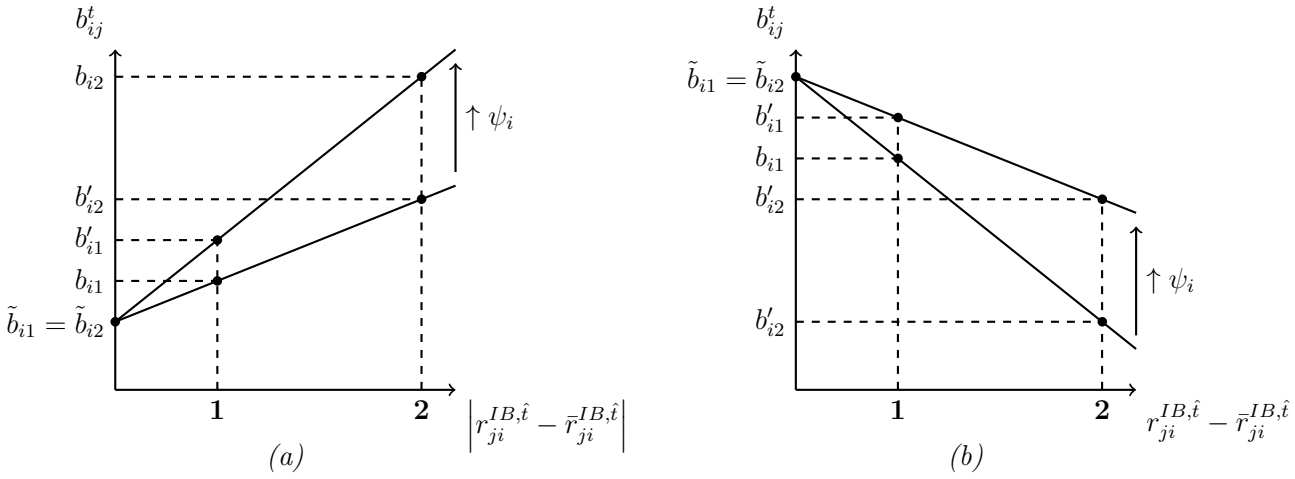

Figure 5:

These requests are then transmitted to creditors who (i) examine how much aggregate liquidity they have on hand to lend out on the interbank market and (ii) decide how to redistribute their aggregate lending amongst borrowers. In our model, we interpret banks' available liquidity in phase as their cash reserves in that period which comprises excess reserves carried over from the previous period ($c_i^{t-1,3}$), dividend payments from their external assets ($e_i^{t-1,2}$) less interest payments to current-period depositors $d_i^{t,1}$[17]. Thus, each bank's liquidity in phase 1 is given by

[17]Note that current liquidity does not include the return on the illiquid investment, z_i^t made at the beginning of the period. This modelling choice was made to represent the maturity mismatch between banks' short-term liabilities (reflected in the negative interest payments to depositors) and long-term assets. Consequently, the return on investment is realised in phase 2 of the model.

$$c_i^{t,1} = c_i^{t-1,3} + r^p \cdot e_i^{t-1,3} - r^d \cdot d_i^{t,1} \tag{15}$$

Once lenders determine how much liquidity they have available for interbank lending, we assume a similar behavioural loan distribution mechanism to borrowers' equally-weighted/non-risk adjusted liquidity requests. That is, lender i allocates $\tilde{l}_{ij}^t = \left(\frac{1}{N_{i,-}^t}\right) \cdot c_i^{t,1}$ for each $j \in \mathcal{N}_{i,-}^t$. The final amount of liquidity transferred from each lender i to its counterparties is then determined by the bilateral liquidity requests b_{ji}^t given in Equation 13 and the provisional amount $\tilde{l}_{ij}^t$ given above. Since, by construction this is determined by the lenders, we assume that bilateral lending is computed using

$$l_{ij}^t = \min\{\tilde{l}_{ij}^t; b_{ji}^t\} \tag{16}$$

Once bilateral loan volumes have been set, lenders proceed to fix the interbank rate offered to each of their counterparties. In our modelling approach, this comprises two primary components: the *counterparty credit risk* of borrowers and the lender's own *liquidity risk*. The former represents the risk to the lender that a particular borrower will not fulfil its contractual obligations i.e. repay the loan. In our model, we treat it as a historical measure whereby lender i uses past information on each borrower j's loan repayment relative to loan provision to determine the counterparty risk premium, $r_{ij}^{CR,t}$. Similar to the rollover risk adjustment factor, lenders locate, for each *current* borrowing counterparty, the last period in which they had the same relationship i.e. $\hat{t}_{ij}^L = \left\{\hat{t} \in [1, t-1] | \Delta d_i^{\hat{t}} \geq 0 \wedge \Delta d_j^{\hat{t}} < 0\right\}$. Given that interbank rates comprise several component factors, we devise the following framework to isolate the counterparty-risk component. At $\hat{t}_{ij}^L$, the lender analyses the counterparty-risk premium set in that period as well as the amount of liquidity loaned out and uses this to construct the *counterparty-risk adjusted* expected return on lending.

$$\tilde{x}_{ij}^{CR,\hat{t}_{ij}^L} = \left(1 + r_{ij}^{CR,\hat{t}_{ij}^L}\right) \cdot l_{ij}^{\hat{t}_{ij}^L} \tag{17}$$

Following this, lenders now determine how much of the interbank rate offered to each borrower in $\hat{t}_{ij}^L$ comprised counterparty risk using

$$\chi_{ij}^{CR,\hat{t}_{ij}^L} = \frac{r_{ij}^{CR,\hat{t}_{ij}^L}}{r_{ij}^{IB,\hat{t}_{ij}^L}} \tag{18}$$

Once past realisations have been passed to the current period as input for the lender, the next step involves observing borrowers' loan repayment behaviour in $\hat{t}_{ij}^L$ and combining this with $\chi_{ij}^{CR,\hat{t}_{ij}^L}$ to obtain the counterparty-risk adjusted repayment rate:

$$r_{ji}^{CR,\hat{t}_{ij}^L} = \chi_{ij}^{CR,\hat{t}_{ij}^L} \cdot \tilde{r}_{ji}^{IB,\hat{t}_{ij}^L}, \quad \text{where} \quad \tilde{r}_{ji}^{IB,\hat{t}_{ij}^L} = \frac{x_{ji}^{\hat{t}_{ij}^L} - l_{ij}^{\hat{t}_{ij}^L}}{l_{ij}^{\hat{t}_{ij}^L}} \tag{19}$$

Finally, the lender reconstructs the counterparty-risk adjusted loan repayment based on the

above values in order to determine how much was *expected* as loan repayment based solely on the borrower's counterparty risk:

$$x_{ji}^{CR,\hat{l}_{ij}^L} = \left(1 + r_{ji}^{CR,\hat{l}_{ij}^L}\right) \cdot l_{ij}^{\hat{l}_{ij}^L} \tag{20}$$

By comparing $\tilde{x}_{ij}^{CR,\hat{l}_{ij}^L}$ and $x_{ji}^{CR,\hat{l}_{ij}^L}$, the lender is able to compare the counterparty risk adjusted loan with the counterparty risk adjusted repayment and use this to construct the counterparty risk premium in the current period, t. We develop a graphical argument similar to the borrower risk adjustment in Figure 5.

4.3.3 Phase 2: Loan repayment and borrower deleveraging

Where phase 1 of the model involved banks opening interbank positions vis-à-vis one another due to an exogenous (liability-side) liquidity shock, In the current phase, banks are now required to close these positions (since we are examining short-term lending). Similar to phase 1 (where deposit shocks drove interbank market activity), we assume that loan refinancing behaviour of borrower banks is driven partially by an exogenous shock to banks' securities portfolios.

Having identified the number of securities to shock, we now turn to the magnitude of the shock i.e. the effect on the marked-to-market price of the selected securities. We incorporate both first-round and second-round effects arising due to aforementioned exogenous shock. The first-round effects are simply the shift in market price from the ex ante value, $p^{\mu,t-1}$ to the ex post price $\tilde{p}^{\mu,t}$. Since the financial state has already been incorporated, we provide the following simplified mechanism for the first-round effects: Each security $\mu = 1, \ldots, n_e^t$ in the shocked portfolio is subject to a percentage reduction in its market price given by $f^{\mu,t} = \mathcal{U}(0, p^{\mu,t-1})$ which, as the support shows, has an upper bound equal to the previous period market price. The current market price of each shocked asset is thus given by

$$\tilde{p}^{\mu,t} = f^{\mu,t} \cdot p^{\mu,t-1} \tag{21}$$

Note that this shock is idiosyncratic since its effect on individual banks will depend on which of the shocked assets it holds in its external assets portfolio. As a result, i's phase 2 balance sheet entry for external assets is updated as:

$$e_i^{t,2} = \sum_{\mu=1}^{n_e^t} s_i^{\mu,t-1} \cdot \tilde{p}^{\mu,t}$$

where s_i^{t-1} denotes i's holdings of the n_e^t selected securities carried over from the previous period and p^t is the vector comprising the market-prices of the n_e^t shocked securities

As for the borrower banks, recall that their borrowing was used to finance the same illiquid investment, thus the first two terms in the equation above are unchanged. Rather than allowing borrowers to withhold a fraction of $q_i^{t,2}$ from the interbank market, we incorporate the notion

of *liquidity hoarding* via a negative term on borrower banks' available liquidity related to the magnitude of the external asset shock. Given that OTC interbank markets entail a bilateral contract between counterparties, our approach does not allow borrowers to default on their loans by keeping a certain amount of liquidity on their balance sheet as a function of borrower-confidence. Thus, borrower liquidity in phase 2 is given by

$$q_i^{t,2} = q_i^{t,1} + r^z z_i^t - \mathbb{E}_t\left[e_i^{t+1,2}\right] \tag{22}$$

where the negative term is interpreted as i's expectation in period t of its portfolio value in $t+1$. We treat this as a martingale i.e. $\mathbb{E}_t\left[e_i^{t+1,2}\right] = e_i^{t,2}$. The expectations operator is used since interest on the portfolio is paid in phase 1 of every period. The bank, using the martingale assumption, predicts a loss in liquidity in period $t+1$ due to current period losses and, deciding to smooth losses in liquidity, decides to devote less to refinancing its interbank positions.

It is here that we incorporate the securities firesale mechanism. Specifically, in order to reduce the possibility of default, we allow borrowers to make up for the difference between available liquidity and repayment obligations by liquidating a portion of their external asset portfolios. This is given by:

$$\widetilde{sell}_i^t = \min\{\min\{0; q_i^{t,2} - b_i^t\}; s_i^t\}$$

where $\widetilde{sell}_i^t$ denotes the provisional volume of external assets that borrower i needs to sell to repay its interbank loans. The outside $\min\{\cdot\}$ function ensures that this amount is constrained by the amount of external assets actually held by the bank in that period i.e. that $0 \leq \tilde{sell}_i^t \leq s_i^t$. Given that the potential buyers of these assets will be investors informed of interbank market characteristics, we use the notion of interbank market confidence developed earlier in the paper to represent the ability of the market to absorb these assets. As a result, the effective amount of securities sold is equal to

$$sell_i^t = \frac{\langle \varphi_i^{l,t-1} \rangle}{\langle \varphi_i^{l,t-2} \rangle} \cdot \widetilde{sell}_i^t \tag{23}$$

The firesale mechanism assumes that all bank securities *within the shocked set* are sold in equal proportion (stemming from the assumption of equally-weighted initial portfolios) with $sell_i^{\mu,t} = \frac{sell_i^t}{n_e^t}$. Borrower banks now use apply the second part of the B-RR to rank creditors according to loan volume (in the stable state) or borrower confidence (in the crisis state) then proceed along this vector in an iterative manner to allocate their aggregate refinancing across their lender neighbourhoods. We begin by setting the initial value for borrower i's aggregate remaining liquidity $x_i^{t,0} = q_i^{t,2} + \sum_{\mu=1}^{n_e^t} \tilde{p}^{\mu,t} \cdot sell_i^{\mu,t}$.

5 Simulations

The simulation stage of the paper is split into two stages: generating the bilayer network then using the network as an initial condition for the agent-based model whereby bank balance sheets are endogenously updated using a simple heuristic based on *confidence* between counterparties. The first stage comprises the following two steps: (i) generating the directed core-periphery network of bilateral interbank exposures using the fitness model developed in section 3.1, (ii) generating the undirected bipartite overlapping portfolio network from section 3.2. The heterogeneous node set along with the neighbours associated to each node are passed as arguments to the initialisation step of the ABM in order to determine the total assets held by the bank and its initial borrower and lender confidence, respectively.

In this section, we provide the simulation methodology used to generate the bilayer network and launch the ABM as well as results of the simulations described above.

5.1 Interbank Network

Generation of the initial interbank network requires three parameters, the power-law exponent and the smallest and largest bank sizes. We choose the following specification: $\{\gamma_a, a_{min}, a_{max}\} = \{2, 5, 200\}$. We follow the general literature on interbank network simulation by generating $N = 250$ banks. In order to obtain the discrete set of fitness parameters, a_i where $i = 1, \ldots 250$, we apply the *inverse transform sampling* method within a Monte Carlo framework by drawing `J = 100,000` random variables from the truncated power-law given in Equation 1. Figure 6 below provides the simulated distribution of bank sizes

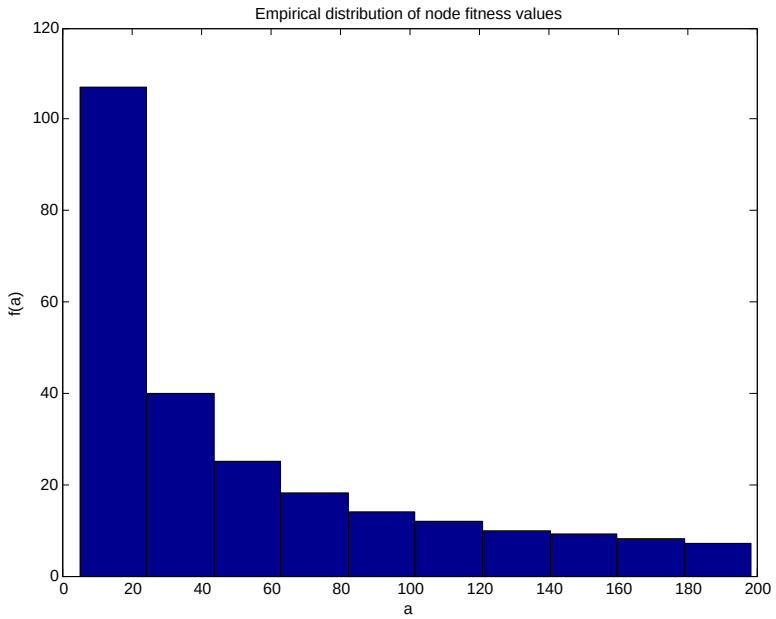

Figure 6: Empirical distribution of node fitness values

The 250-element vector of bank sizes is then passed to the probability function (Eq. 2) to populate the 250^2 element probability matrix denoting the probability that a given pairs of banks ij will form an edge[18]. In order to prevent isolated nodes (which occurs for smaller nodes whose probability of forming an edge is small) resulting in a *disconnected* network, we develop a contingency by which a disconnected node will form a link to a randomly-selected node in the top quintile of a (comprising 50 banks). In this way, we conserve the core-periphery structure of the network. We simulate `K = 100` statistical realisations of the network and report the minimum, maximum , mean and variance across these for a number of network measures[19] in table 1 below:

Table 1: Measures of simulated interbank networks across 100 statistical realisations

Measure	Minimum	Maximum	Mean	Standard Deviation
Number of edges	4212.00	4614.00	4401.26	81.03
Density	0.068	0.074	0.071	0.001
Average degree	16.85	18.46	17.61	0.32
Average path length	2.32	2.41	2.37	0.02
Diameter	4.00	6.00	4.90	0.15
Global clustering	0.10	0.12	0.11	0.00
Average local clustering	0.22	0.28	0.25	0.01

Using the GEPHI graph visualisation software, we present the median (in terms of number of edges) simulated network below

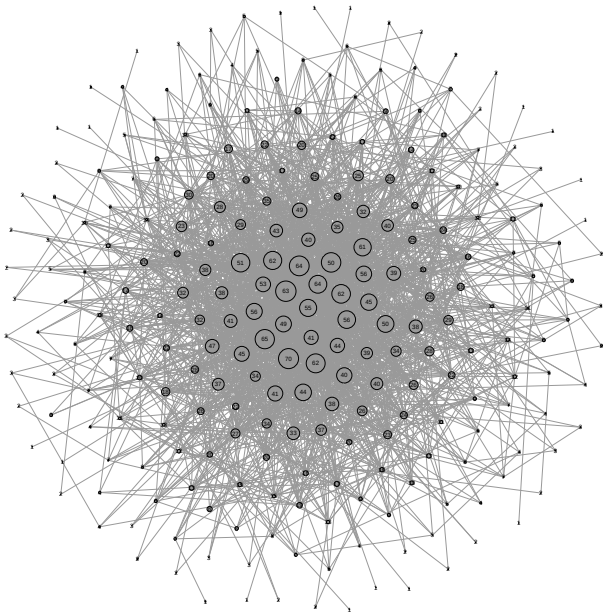

Figure 7: Median network with 4408 edges

[18]In order to reduce the computational burden, we take advantage of the fact that the matrix is (i) symmetric and (ii) free of self-loops by applying the probability function to node pairs *below* the main diagonal. As a result, the algorithm cycles through $N(N-1)/2 = 31{,}125$ values rather than the full $N^2 = 62{,}500$. Adding the generated matrix and its transpose gives us the final adjacency matrix

[19]To compute these, we make heavy use of the MIT 'MATLAB tools for network analysis' toolbox, available at http://strategic.mit.edu/downloads.php?page=matlab_networks.

The labels denote the degree of each edge exemplifying the presence of a highly-interconnected *core* while moving away from the core (from the centre outwards) results in less dense linkages. Nodes on the periphery display very low degree and are connected primarily to core banks. Thus, our simulation successfully replicates the tiered network structure that characterises interbank markets.

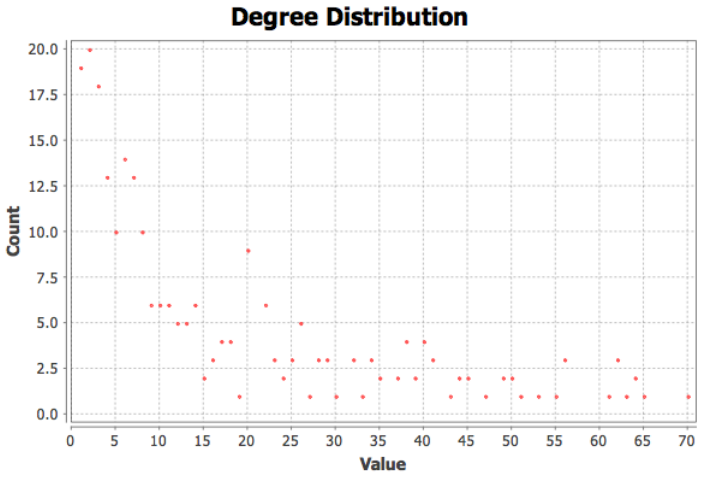

Figure 8: Degree distribution of median-edge network

5.1.1 Overlapping portfolio network

5.2 ABM

The Agent-Based Model combines calibrated parameters for the heterogenous initial balance sheets of the banks and the stochastic shock regimes with the output from the network generation stage above. Specifically, the node fitness values a_i define banks' total assets which is then used to create the balance sheet parameters via the α and β calibrations given in Table 2. Similarly, the in (out) going linkages of the networks define the initial borrower (lender) confidence neighbourhoods. Moreover, given that the dynamics of the model is driven by exogenous shocks to the asset and liability side of the balance sheet, Table 2 provides the calibrations determining whether the economy is in a stable or crisis state.

Table 2: Calibrated parameters for the Agent-Based Model

Parameter	Definition	Value
	Initial balance sheet weights	
α	external asset fraction	0.9
β	deposit fraction	0.92
	Shock parameters	
(μ_1^s, σ_1^s)	Stable state deposit shock parameters	TBD
(μ_1^c, σ_1^c)	Crisis state deposit shock parameters	TBD
(μ_2^s, σ_2^s)	Stable state external asset shock parameters	TBD
(μ_2^c, σ_2^c)	Crisis state external asset shock parameters	TBD

6 Results

Author's note to NBB recruitment committee: The MATLAB code for the ABM is currently being implemented. As this is a contribution in itself, I have included a sample of the main scripts (network generation and ABM) as an additional attachment with my application

References

Acemoglu, Daron, Asuman Ozdaglar, and Alireza Tahbaz-Salehi (2015), "Systemic risk and stability in financial networks." American Economic Review, 105, 564–608.

Afonso, Gara, Anna Kovner, and Antoinette Schoar (2013), "Trading partners in the interbank lending market." FRB of New York Staff Report.

Ait-Sahalia, Yacine, Jochen Andritzky, Andreas Jobst, Sylwia Nowak, and Natalia Tamirisa (2012), "Market response to policy initiatives during the global financial crisis." Journal of International Economics, 87, 162–177.

Allen, Franklin and Ana Babus (2009), "Networks in finance." In The network challenge: strategy, profit, and risk in an interlinked world (Paul R Kleindorfer and Yoram Wind, eds.), 367–382, Pearson Prentice Hall.

Anand, Kartik, Prasanna Gai, Sujit Kapadia, Simon Brennan, and Matthew Willison (2013), "A network model of financial system resilience." Journal of Economic Behavior & Organization, 85, 219–235.

Axelrod, Robert M (1997), The complexity of cooperation: Agent-based models of competition and collaboration. Princeton University Press.

Bech, Morten L and Enghin Atalay (2010), "The topology of the federal funds market." Physica A: Statistical Mechanics and its Applications, 389, 5223–5246.

Boss, Michael, Helmut Elsinger, Martin Summer, and Stefan Thurner 4 (2004), "Network topology of the interbank market." Quantitative Finance, 4, 677–684.

Brunnermeier, Markus K and Lasse Heje Pedersen (2009), "Market liquidity and funding liquidity." Review of Financial studies, 22, 2201–2238.

Caccioli, Fabio, J Doyne Farmer, Nick Foti, and Daniel Rockmore (2015), "Overlapping portfolios, contagion, and financial stability." Journal of Economic Dynamics and Control, 51, 50–63.

Caccioli, Fabio, Munik Shrestha, Cristopher Moore, and J Doyne Farmer (2014), "Stability analysis of financial contagion due to overlapping portfolios." Journal of Banking & Finance, 46, 233–246.

Caldarelli, Guido, Andrea Capocci, Paolo De Los Rios, and Miguel A Muñoz (2002), "Scale-free networks from varying vertex intrinsic fitness." Physical review letters, 89, 258702.

Cifuentes, Rodrigo, Gianluigi Ferrucci, and Hyun Song Shin (2005), "Liquidity risk and contagion." Journal of the European Economic Association, 3, 556–566.

Cocco, Joao F, Francisco J Gomes, and Nuno C Martins (2009), "Lending relationships in the interbank market." Journal of Financial Intermediation, 18, 24–48.

Colander, David, Peter Howitt, Alan Kirman, Axel Leijonhufvud, and Perry Mehrling (2008), "Beyond dsge models: toward an empirically based macroeconomics." The American Economic Review, 236–240.

Craig, Ben and Goetz Von Peter (2014), "Interbank tiering and money center banks." Journal of Financial Intermediation.

Eisenschmidt, Jens and Jens Tapking (2009), "Liquidity risk premia in unsecured interbank money markets." Technical report, European Central Bank.

Farmer, J Doyne and Duncan Foley (2009), "The economy needs agent-based modelling." Nature, 460, 685–686.

Fricke, Daniel and Thomas Lux (2014), "Core–periphery structure in the overnight money market: evidence from the e-mid trading platform." Computational Economics, 1–37.

Gai, Prasanna and Sujit Kapadia (2010), "Contagion in financial networks." Proceedings of the Royal Society A: Mathematical, Physical and Engineering Science, 466, 2401–2423.

Geanakoplos, John (2010), "The leverage cycle." In NBER Macroeconomics Annual 2009, Volume 24, 1–65, University of Chicago Press.

Haldane, Andrew G (2009), "Rethinking the financial network." Speech delivered at the Financial Student Association, Amsterdam, April.

Heider, Florian, Marie Hoerova, and Cornelia Holthausen (2015), "Liquidity hoarding and interbank market spreads: The role of counterparty risk." Journal of Financial Economics, 118, 336–354.

Huang, Xuqing, Irena Vodenska, Shlomo Havlin, and H Eugene Stanley (2013), "Cascading failures in bi-partite graphs: model for systemic risk propagation." Scientific reports, 3.

in't Veld, Daan and Iman van Lelyveld (2014), "Finding the core: Network structure in interbank markets." Journal of Banking & Finance, 49, 27–40.

Iori, Giulia, Giulia De Masi, Ovidiu Vasile Precup, Giampaolo Gabbi, and Guido Caldarelli (2008), "A network analysis of the italian overnight money market." Journal of Economic Dynamics and Control, 32, 259–278.

Iori, Giulia, Rosario N Mantegna, Luca Marotta, Salvatore Miccichè, James Porter, and Michele Tumminello (2015), "Networked relationships in the e-mid interbank market: A trading model with memory." Journal of Economic Dynamics and Control, 50, 98–116.

Jorion, Philippe and Gaiyan Zhang (2009), "Credit contagion from counterparty risk." The Journal of Finance, 64, 2053–2087.

Langfield, Sam, Zijun Liu, and Tomohiro Ota (2014), "Mapping the uk interbank system." Journal of Banking & Finance, 45, 288–303.

Lux, Thomas (2015), "Emergence of a core-periphery structure in a simple dynamic model of the interbank market." Journal of Economic Dynamics and Control, 52, A11 – A23.

Michaud, François-Louis and Christian Upper (2008), "What drives interbank rates? evidence from the libor panel." BIS Quarterly Review, March.

Montagna, Mattia and Thomas Lux (2013), "Hubs and resilience: towards more realistic models of the interbank markets." Technical report, Kiel Working Paper.

Nier, Erlend, Jing Yang, Tanju Yorulmazer, and Amadeo Alentorn (2007), "Network models and financial stability." Journal of Economic Dynamics and Control, 31, 2033–2060.

Schwarz, Krista (2015), "Mind the gap: Disentangling credit and liquidity in risk spreads."

Schweitzer, Frank, Giorgio Fagiolo, Didier Sornette, Fernando Vega-Redondo, Alessandro Vespignani, and Douglas R White (2009), "Economic networks: The new challenges." Science, 325, 422–425.

Soramäki, Kimmo, Morten L Bech, Jeffrey Arnold, Robert J Glass, and Walter E Beyeler (2007), "The topology of interbank payment flows." Physica A: Statistical Mechanics and its Applications, 379, 317–333.

Summer, Martin (2013), "Financial contagion and network analysis." Annu. Rev. Financ. Econ., 5, 277–297.

Taylor, John B. and John C. Williams (2009), "A black swan in the money market." American Economic Journal: Macroeconomics, 1, 58–83.

Tesfatsion, Leigh and Kenneth L Judd (2006), Handbook of computational economics volume 2: Agent-based computational economics, volume 2. Elsevier.

Upper, Christian (2011), "Simulation methods to assess the danger of contagion in interbank markets." Journal of Financial Stability, 7, 111–125.

7 Network theory

7.1 Basic definitions

A useful property of directed networks that can be derived from the adjacency matrix is the in- and out-degree of each node which represent the number of incoming and outgoing links, respectively:

Definition 1. *The in- and out- degree, d_i^{in} and d_i^{out} of a node, $i \in \mathcal{N}$ are given by:*

$$d_i^{in} = \sum_{j=1}^{N} a_{ji} = (\mathcal{A}^\top)_i \cdot \mathbf{1} \quad d_i^{out} = \sum_{j=1}^{N} a_{ij} = (\mathcal{A})_i \cdot \mathbf{1}$$

Where $A^\top$ is the transpose of A[20], $(\mathcal{A})_i$ is the i^{th} row of $\mathcal{A}$ and $\mathbf{1}$ is an N-dimensional column vector $(1, \dots 1)^\top$.

For each node i, we distinguish between its in- and out-degree as this determines its initial neighbourhood of counterparties for whom i serves as a lender or borrower, denoted by the sets $\mathcal{N}_i^{l,0}(\mathcal{G}) = \{j : a_{ij} = 1\}$ and $\mathcal{N}_i^{b,0}(\mathcal{G}) = \{j : a_{ji} = 1\}$ whose cardinalities are given by the out- and in-degree, respectively.

7.2 Bipartite networks

7.3 Global network measures

Average path length is a measure that takes the average of the shortest path (referred to as the *geodesic* in the graph theory literature) of the network $\mathcal{G} = (\mathcal{N}, \vec{\mathcal{E}})$ between all pairs of nodes, $i, j \in \mathcal{N}$. In a directed network, a path between i and j is defined as a sequence of edges $\{i_1, i_2\}, \{i_2, i_3\} \dots \{i_{N-1}, i_N\}$ such that $i_1 = i$ and $i_N = j$ and each node in the sequence $i_1 \dots i_N$ is distinct. These results can be summarised in the an $N \times N$*geodesic distance matrix*, $(\mathcal{G}^{\mathcal{IB}})$ where the elements d_{ij} of $D(\cdot)$ represent the path length between ij.

Density measures how *connected* the network $(\mathcal{N}, \vec{\mathcal{E}})$ is relative to the complete graph constructed on $\mathcal{N}$ (i.e. the graph with the maximum number of edges). In the directed case, this is given by:

$$D = \frac{E}{N(N-1)} \tag{24}$$

Clustering coefficient is defined in **?** as the probability that two incident edges, $ij \in \vec{\mathcal{E}}$ are completed by a third one to form a triangle. **?** extends the framework to binary (i.e. unweighted) directed networks. Given a node i, the product $a_{ij}a_{jk}a_{ik}$ denotes any one of the 8 possible triangles that i can form with its neighbours j and k. Consequently, the *local clustering coefficient* of i is

[20] We adopt the convention that the i^{th} row (column) represents node i's outgoing (incoming) links.

defined as the number of directed triangles *actually* formed by i (t_i^D) divided by the total number of *potential* triangles i could form (T_i^D) . This is expressed mathematically as,

$$\begin{aligned} C_i^D(A) &= \frac{t_i^D}{T_i^D} = \frac{\frac{1}{2}\sum_j \sum_k (a_{ij} + a_{ji})(a_{ik} + a_{ki})(a_{jk} + a_{kj})}{[d_i^{tot}(d_i^{tot} - 1) - 2d_i^{\leftrightarrow}]} \\ &= \frac{(A + A^\top)^3_{ii}}{2\,[d_i^{tot}(d_i^{tot} - 1) - 2d_i^{\leftrightarrow}]} \end{aligned}$$